PREDICTION OF EQUIVALENT CIRCUIT OF MULTI-LAYER CERAMIC CAPACITOR BASED ON COUPLED TRANSMISSION LINE THEORY

[1]JIWOON JEON, [2]JONGHYEON KIM, [3]BO PU, [4]WANSOO NAH

[1,2,3,4]SungKyunKwan University College of Information and Communication Engineering
E-mail: anbs19@naver.com, ocdongza@gmail.com, bob.pu@hotmail.com, wsnah@skku.edu

Abstract- The equivalent circuit modeling techniques of MLCC (Multi-Layer Ceramic Capacitor) have been introduced in many papers. However these techniques need measured data, such as S-parameters to extract circuit parameters of MLCC, which is possible only after fabrication. This paper proposes the modeling method which does not need the experimentally measured data and only needs both structure and material data which can be determined at design stage. To verify the validness of the proposed circuit model, an MLCC which has 47nF, X7R and 1206 size is used in measurement to compare with proposed model. It is confirmed that the predicted impedance from the proposed equivalent circuit are quite perfectly matched with the measured results.

Keywords- Coupled Transmission Line, Equivalent Circuit, Modeling, MLCC, Polishing, Prediction

I. INTRODUCTION

MLCC (Multi-Layer Ceramic Capacitor) is the most widely used passive component in electronics industry because of its various applications such as DC blocking, decoupling and filtering etc. With its importance on the microelectronic circuits, many papers have been published for an equivalent circuit model of MLCC. However, the modeling techniques introduced in these papers need measured data, such as S-parameter to get the circuit parameters of MLCC, which is possible only after the fabrication of the MLCC. This can causes not only time loss but material loss at manufacture and measurement stage. This paper proposes modeling method to get an equivalent circuit of the MLCC, which does not need the experimentally measured data showing that the impedance characteristics of N-Layer Capacitor can be expressed in mathematical form in terms of its structure and material dat. From this predicted impedance, equivalent circuit of the MLCC is obtained by simple parameter extraction.

MLCC can be divided into three regions, which are end, nonoverlap and overlap region noticing that nonoverlap and overlap region are sub regions of electrode region. These regions are rectangular wires which can be modeled in terms of distributed elements using PEEC (Partial Element Equivalent Circuit) method. Considering skin effect and fringing field, the circuit parameters such as resistance, inductance, capacitance and conductance are modeled as the functions of frequency. From these results, the end and nonoverlap regions are modeled as a series combination of resistance and inductance but another mutual inductance should be included in the nonoverlap region. The overlap region is modeled as coupled transmission lines, and a set of differential equations can be used to describe voltages and currents of transmission lines.

To verify the validness of proposed circuit model, an MLCC which has capacitance of 47nF, temperature characteristic of X7R and size of 1206 is used in measurement and de-embedding is also carried out to subtract the elements of PCB. The structure data is obtained from polishing to get the predicted impedance of the MLCC.

The modeling procedures of N-Layer Capacitor is described in Section Ⅱ, and measurement is discussed in Section Ⅲ. Finally, a concluding remarks is presented in Section Ⅳ.

II. N-LAYER CAPACITOR

A typical structure of an MLCC is shown in Fig. 1. End region represents external current path used for soldering, overlap region is coupled capacitive region which forms

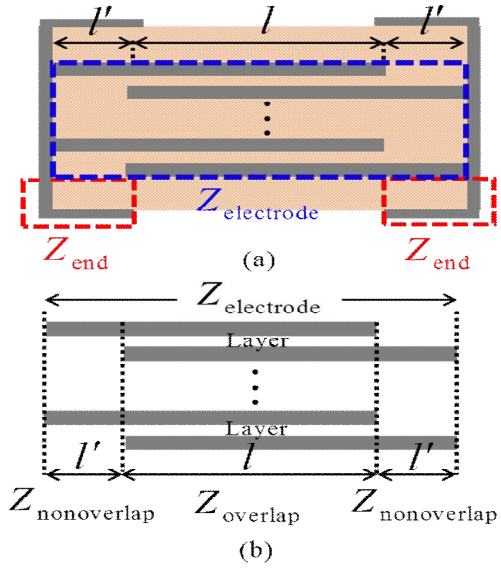


Fig. 1. (a) Cross sectional view of MLCC. (b) Configuration of electrode region.

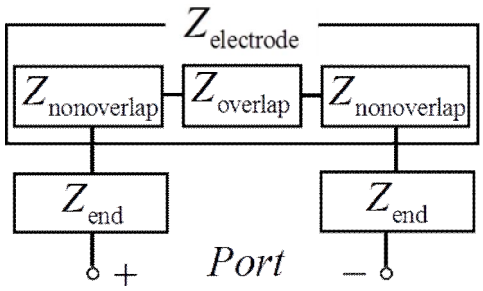


Fig. 2. Systematical block model of MLCC.

Layers which are referred to as Z_{end}, $Z_{overlap}$ respectively. The nonovelap region is an channel between end and overlap region referred to as $Z_{overlap}$. Total block model of MLCC can be systematically depicted as shown in Fig. 2, where total series impedance is $Z_{MLCC} = Z_{electrode} + 2Z_{end}$ [2]

A.Circuit Parameters of rectangular wire

An isolated rectangular wire which has width w, thickness t, length l is shown in Fig. 3(a) to describe resistance and self-partial inductance in terms of its w, t, l and frequency. Also parallel two rectangular wires are shown in Fig. 3(b) to obtain the mutual inductance, capacitance and conductance in terms of their structure and material data. In these configurations, the circuit parameters such as resistance (R), inductance (L), mutual inductance (M), capacitance (C) and conductance (G) can be obtained from.

$$Z_{int} = \sqrt{\left(\frac{1}{\sigma w t}\right)^2 + \left((1+j)\frac{\sqrt{\omega^2\mu}}{p\sqrt{2\sigma\omega_0}}\right)^2} \quad (\Omega/\mathrm{m}) \quad (1)$$

$$R = real\{Z_{int}\} \times l \quad (\Omega) \quad (2)$$

where Z_{int} is the internal impedance of the rectangular wire in Fig. 3(a), k_p is factor of proximity effect, k_r is factor of roughness effect, ω_0 is a particular frequency (rad/s) chosen well above the onset of the skin effect and p is the perimeter of wire. In this paper, k_p and k_r is set to 1 assuming that both effects are ignored.

Self-partial inductance of wire is

$$L = \frac{\mu_0 l}{2\pi}\left[\ \ln\left(u + \sqrt{(u)^2+1}\right) + u\ln\left(\frac{1}{u} + \sqrt{\left(\frac{1}{u}\right)^2+1}\right)\right. \quad (3)$$

$$\left. + \frac{1}{3}\left(u^2 + \frac{1}{u} - \frac{(u^2+1)^{1.5}}{u}\right)\right] - 2\times10^{-7}\frac{t}{w}l + imag\{Z_{int}\} \quad (\mathrm{H})$$

where $u = l/w$ which is "aspect ratio" and the last term means the internal inductance which decreases as the frequency increase.

Mutual inductance between parallel two rectangular

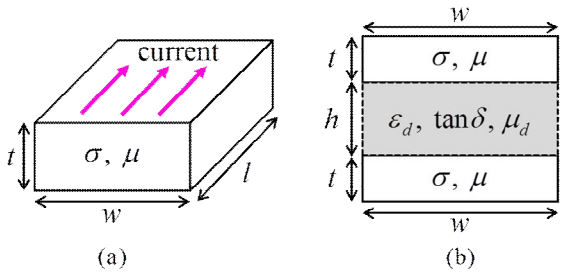


Fig. 3. (a) Isolated rectangular wire. (b) Cross sectional view of parallel two rectangular wires.

wires which have same structure is

$$M = \frac{\mu_0}{2\pi} l\left(\ln\frac{2l}{D} - 1\right), \quad l \gg D \ (\mathrm{H}) \quad (4a)$$

$$\ln D = -\frac{25}{12} + \frac{1}{2(w_1t_1)(w_2t_2)}\sum_{i=1}^{4}\sum_{j=1}^{4}(-1)^{i+j} f(q_i, r_j) \quad (4b)$$

$$f(q,r) = \left(\frac{q^2r^2}{4} - \frac{q^4}{24} - \frac{r^4}{24}\right)\ln\left(q^2+r^2\right) + \frac{q^3 r}{3}\tan^{-1}\frac{r}{q} + \frac{qr^3}{3}\tan^{-1}\frac{q}{r} \quad (4c)$$

$$\begin{pmatrix} q_1 = a - \frac{w_1}{2} - \frac{w_2}{2} & r_1 = b - \frac{t_1}{2} - \frac{t_2}{2} \\ q_2 = a + \frac{w_1}{2} - \frac{w_2}{2} & r_2 = b + \frac{t_1}{2} - \frac{t_2}{2} \\ q_3 = a + \frac{w_1}{2} + \frac{w_2}{2} & r_3 = b + \frac{t_1}{2} + \frac{t_2}{2} \\ q_4 = a - \frac{w_1}{2} + \frac{w_2}{2} & r_4 = b - \frac{t_1}{2} + \frac{t_2}{2} \end{pmatrix} \quad (4d)$$

where D is the GMD (Geometrical Mean Distance) given in (4b)-(4d). In configuration of Fig. 3(b), the value a and b are given as 0, h respectively.

Finally, capacitance and conductance of the parallel two rectangular wires are described in (5)-(6).

$$C = \frac{\varepsilon_0\varepsilon_d(w\times l)}{d} + 2l\times\frac{\varepsilon_0\varepsilon_d}{2\pi}\ln\frac{2l\pi}{d} \quad (\mathrm{F}) \quad (5)$$

$$G = \omega C\tan\delta \quad (\mathrm{S}) \quad (6)$$

In (5), the first term represents the parallel plate capacitance when the plates have infinite area while the second term means "Fringing capacitance" at the edge of wires which can be calculated by conformal mapping. In (6), $\tan\delta$ is the loss tangent of dielectric between the wires.

B. N(odd)-Layer Capacitor

The modeling process of end region is shown in Fig. 4. With this configuration and (1)-(3), end region can be modeled as

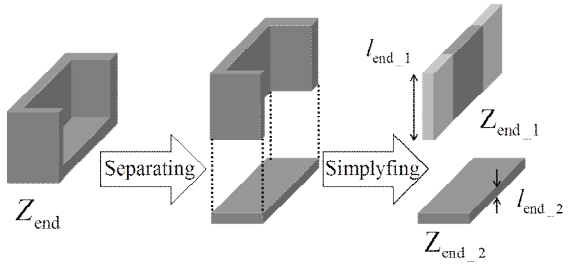


Fig. 4. Modeling process of end region.

$$Z_{\text{end}} = \left(R_{end_1} + j\omega L_{end_1}\right) l_{end_1} + \left(R_{end_2} + j\omega L_{end_2}\right) l_{end_2} \quad (7)$$

where

R_{end_1} = Resistance of the sub-region1 (Ω/m)

L_{end_1} = Inductance of the sub-region1 (H/m)

R_{end_2} = Resistance of the sub-region2 (Ω/m)

L_{end_2} = Inductance of the sub-region2 (H/m)

noticing that both left and right end region have same impedance as shown in Fig. 1(a).

The overlap region can be modeled as coupled transmission lines which have N layers and (N+1) plates because two plates forms one layer. The equivalent circuit of coupled transmission lines is shown in Fig. 5. Assuming that proximity effect is ignored, Fig. 5(a) can be simplified to Fig. 5(b). All circuit parameters are expressed in distributed elements. Configuration of N(odd)-layer capacitor is shown in Fig. 6. From Fig. 6, the plates of left $(1,3,\cdots,\text{N})$ are connected in parallel sharing node A, while the plates of right $(2,4,\cdots,\text{N+1})$ are connected in parallel sharing node.

B. Therefore, the voltage of node A and B can

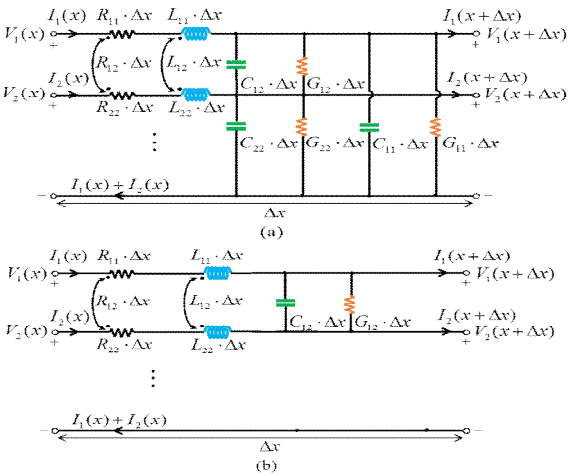


Fig. 5. (a) Equivalent circuit of coupled transmission line for overlap region. (b) Simplified equivalent circuit.

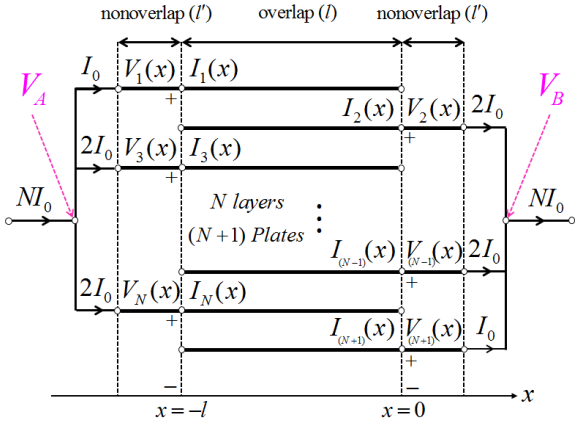


Fig. 6. Configuration of N(odd)-layer capacitor.

be expressed as (8b), (8c).

$$\text{Total current} = I_0 + 2I_0\left(\frac{N-1}{2}\right) = NI_0 \quad (8a)$$

$$V_A = V_1(-l) + I_0 Z_{\text{nonoverlap_1}} = V_3(-l) + 2I_0 Z_{\text{nonoverlap_3}} \vdots = V_{\text{N}}(-l) + 2I_0 Z_{\text{nonoverlap_N}} \quad (8b)$$

$$V_B = V_2(0) - 2I_0 Z_{\text{nonoverlap_2}} = V_4(0) - 2I_0 Z_{\text{nonoverlap_4}} \vdots = V_{(\text{N+1})}(0) - I_0 Z_{\text{nonoverlap_(N+1)}} \quad (8c)$$

$$Z_{electrode} = \frac{V_A - V_B}{NI_0} \quad (8d)$$

The impedance of electrode region can be calculated as described in (8d) because impedance is given as the ration the voltage difference to total current.

In this paper, $V_1(x)$ and $V_2(x)$ are chosen to get the voltage difference between node A and B. This indicates that it needs only two voltages and two currents solved from differential equations (18) based on telegrapher equations.

$$\frac{d}{dx}V_1(x) = -R_{11}I_1(x) - j\omega\sum_{i=1}^{N+1} L_{1i}I_i(x) \quad (9a)$$

$$\frac{d}{dx}V_2(x) = -R_{22}I_2(x) - j\omega\sum_{i=1}^{N+1} L_{2i}I_i(x) \quad (9b)$$

$$\frac{d}{dx}I_1(x) = -\{G_{12}V_1(x) - G_{12}V_2(x)\} - j\omega\{C_{12}V_1(x) - C_{12}V_2(x)\} = -Y_m \cdot \{V_1(x) - V_2(x)\} \quad (9c)$$

$$\frac{d}{dx}I_2(x) = -\{-(G_{21}+G_{23})V_1(x) + (G_{21}+G_{23})V_2(x)\} - j\omega\{-(C_{21}+C_{23})V_1(x) + (C_{21}+C_{23})V_2(x)\} = -2Y_m \cdot \{V_1(x) - V_2(x)\} \quad (9d)$$

where

$Y_m = G_{pq} + j\omega C_{pq}$, $|p-q| = 1$

With the calculations of self and mutual inductances,

(9a) and (9b) can be rewritten as in (10a) and (10b) respectively.

$$\frac{d}{dx}V_1(x) = -R_{11}I_1(x) - j\omega\left(L_{11} + 2\sum_{i=2}^{(N+1)/2} L_{1(2i-1)}\right)I_1(x)$$

(10a) $$-j\omega\left(\sum_{i=1}^{(N-1)/2} L_{1(2i)} + \frac{1}{2}L_{1(N+1)}\right)I_2(x)$$
$$= -Z_{11}I_1(x) - Z_{12}I_2(x)$$

$$\frac{d}{dx}V_2(x) = -R_{22}I_2(x) - j\omega\left(L_{21} + 2\sum_{i=2}^{(N+1)/2} L_{2(2i-1)}\right)I_1(x)$$

(10b) $$-j\omega\left(\sum_{i=1}^{(N-1)/2} L_{2(2i)} + \frac{1}{2}L_{2(N+1)}\right)I_2(x)$$
$$= -Z_{21}I_1(x) - Z_{22}I_2(x)$$

The impedance of electrode region can be expressed in terms of Z_{11}, Z_{12}, Z_{21}, Z_{22} and Y_m which are calculated from (1)-(6). The impedance of electrode region from the solution for (9)-(10) are given by

$$Z_{overlap} = \frac{V_1(-l) - V_2(0)}{NI_0} \quad (11)$$
$$= \frac{(Z_{11} - 2Z_{12})}{2N(Z_{11} + 2Z_{22} - 2Z_{12} - Z_{21})\sinh\gamma l}$$
$$\times [\ \{(Z_{11} - Z_{21}) + 2(Z_{22} - Z_{12})e^{-\gamma l}\}\left(\frac{e^{\gamma l}}{\gamma} - l\right)$$
$$+\{(Z_{11} - Z_{21}) + 2(Z_{22} - Z_{12})e^{\gamma l}\}\left(\frac{e^{-\gamma l}}{\gamma} + l\right)\ ] + \frac{2}{N}Z_{12}l$$
$$-\frac{(Z_{21} - 2Z_{22})}{2N(Z_{11} + 2Z_{22} - 2Z_{12} - Z_{21})\sinh\gamma l}$$
$$\times [\ \{(Z_{11} - Z_{21}) + 2(Z_{22} - Z_{12})e^{-\gamma l}\}\left(\frac{1}{\gamma}\right)$$
$$+\{(Z_{11} - Z_{21}) + 2(Z_{22} - Z_{12})e^{\gamma l}\}\left(\frac{1}{\gamma}\right)\ ]$$

where
$$\gamma^2 = Y_m(Z_{11} + 2Z_{22} - 2Z_{12} - Z_{21})$$

The configuration of nonoverlap region is shown in Fig. 7.

Because $V_1(x)$ and $V_2(x)$ are chosen for calculations, $Z_{\text{nonoverlap_1}}$ and $Z_{\text{nonoverlap_2}}$ should be used. From Fig. 7, these impedance can be obtained.

$$Z_{\text{nonoverlap_1}} = R_{\text{nonoverlap_1}}l' + j\omega\left(L_{\text{nonoverlap_1}} + \sum_{i=2}^{(N+1)/2} L_{\text{nonoverlap_1(2i-1)}}\right)l' \quad (12a)$$

$$Z_{\text{nonoverlap_2}} = R_{\text{nonoverlap_2}}l' + j\omega\left(L_{\text{nonoverlap_2}} + \sum_{i=2}^{(N+1)/2} L_{\text{nonoverlap_1(2i)}}\right)l' \quad (12b)$$

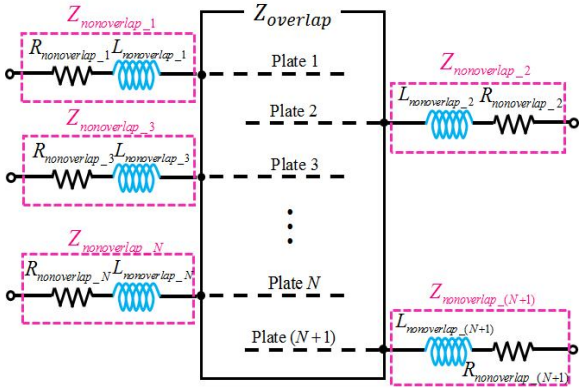


Fig. 7. Configuration of nonoverlap region of N(odd)-Layer capacitor.

where L_{mn} means the mutual inductance.

Finally, the predicted impedance of MLCC is

$$Z_{\text{MLCC}} = Z_{\text{electrode}} + 2Z_{\text{end}} \quad (13)$$

$$Z_{\text{electrode}} = \frac{Z_{\text{nonoverlap_1}}}{N} + \frac{V_1(-l) - V_2(0)}{NI_0} + \frac{2Z_{\text{nonoverlap_2}}}{N}$$

C. N(even)-Layer Capacitor

The impedance of N(even)-Layer Capacitor can be modeled as same procedure of N(odd)-Layer Capacitor.

III. MEASUREMENT

A. Polishing

The notations which should be specified by polishing are shown in Fig. 8 and the polishing results are shown in Fig. 9 captured by optical microscope. Measured structure data are listed in Table Ⅰ and material data are also listed in Table Ⅰ from.

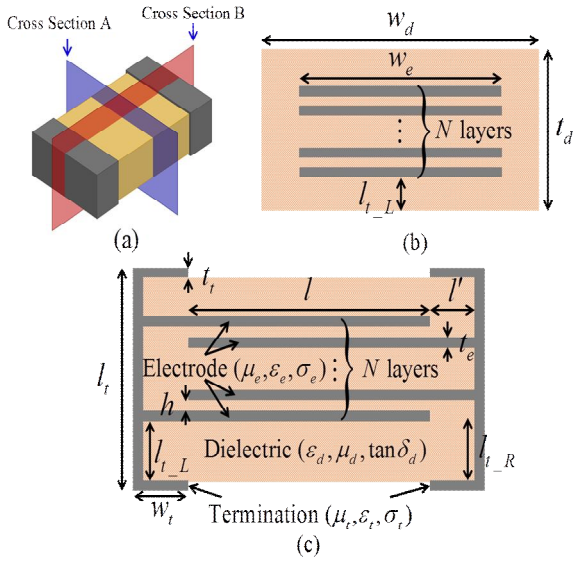


Fig. 8. Notations of main structure and material data (a) Cross section A and B. (b) Cross sectional view of A. (c) Cross sectional view of B.

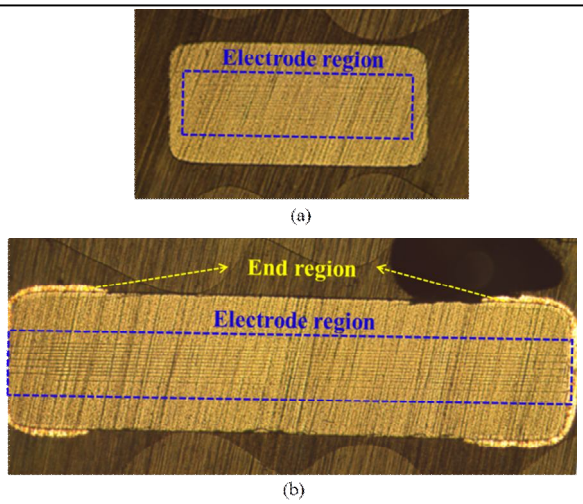


Fig. 9. Captured picture by optical microscope. (a) Cross section A. (c) Cross section B.

B. S-parameters

The MLCC used in this paper is 47nF of capacitance, X7R of temperature characteristics and size of 1206. Using the parameters listed in Table Ⅰ, the predicted impedance can be obtained by calculations in Section Ⅱ. To verify the validness of this result, measurement of S-parameters is carried out to get Z_{11} of the MLCC. Measurement setup is shown in Fig. 10. The measurement is performed using Agilent E5061B Network Analyzer and frequency range is from 300KHz to 3GHz.

However, Z_{11} includes the elements of PCB that are not exact impedance of the MLCC. Therefore de-embedding should be calculated after measurement. In this paper, simple de-embedding techniques is used and this result is compared with proposed model.

Table I. Main structure and material data used in this paper

N	ε_e	μ_e	σ_e (S/m)
10	1	1	5.8×10^7
ε_t	μ_t	σ_t (S/m)	ε_d
1	1	5.8×10^7	2000
μ_d	$\tan\delta$	l_t (mm)	w_t (mm)
1	0.01	0.8652	0.5643
t_t (mm)	t_e (mm)	l_{t_L} (mm)	l_{t_R} (mm)
0.0376	0.0056	0.2908	0.2908
l (mm)	l' (mm)	t_d (mm)	h_e (mm)
2.53	0.2257	0.79	0.01537
w_e (mm)	w_d (mm)	ω_0	h_t (mm)
1.2794	1.65	3×10^9	1.7252
electrode		end	
Cu		Cu	
dielectric			
$BaTiO_3$			

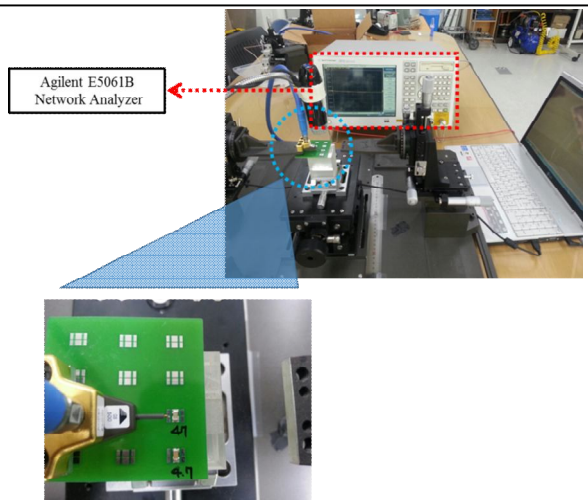


Fig. 10. Photograph of measurement setup.

C. Discussion

The magnitude and phase of impedance proposed model and measurement are shown in Fig. 11. Noticing that the calculation of proposed model is performed by MATLAB, proposed predicted impedance is matched quite perfect compared with the measured one. Finally, the equivalent circuits can be made by extracting ESR , ESL and C_{eq} which is equivalent series capacitance. These values are listed in Table Ⅱ compared with each other. ESR is extracted at SRF (Self Resonant Frequency), ESL is extracted at 300MHz and C_{eq} is calculated at 1MHz.

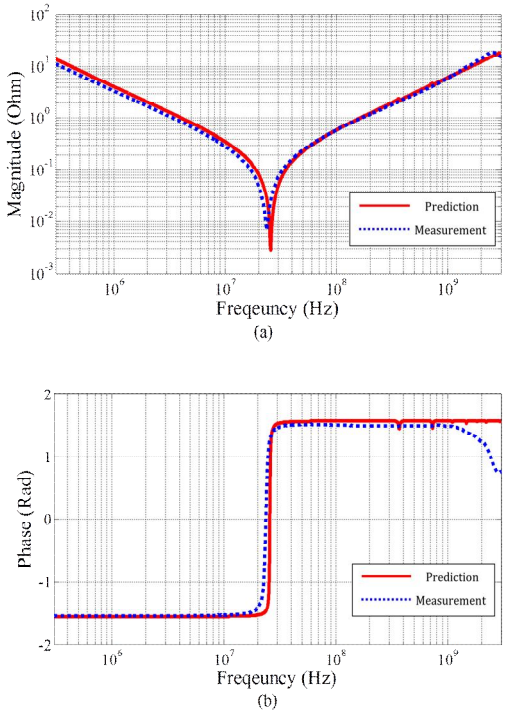


Fig. 11. Comparisons predicted impedance with measured impedance. (a) Magnitude. (b) Phase.

Tabel II. SRF, ESR, SEL and equivalent capacitance

	SRF	ESR	ESL	C_{eq}

Prediction	25.8MHz	2.9mΩ	1.007nH	38.3nF
Measure-ment	23.7MHz	6.8mΩ	1.05nH	41.1nF

CONCLUSION

This paper demonstrates the equivalent circuit modeling of MLCC which can predict the impedance based on coupled transmission line theory. It was confirmed that proposed model matched well with measured one by comparing prediction with measurement. Noticing that the proposed model took only less than one second, it could be useful to design a MLCC because it does not need measurement of device. In addition, with some useful assumption for calculations of differential equations, we could reduce the time to solve those equations without any optimization.

REFERENCES

[1] Jeong-Oh Hong, Sng-Hyuk kim, and Kan-Heon Hur, "Development history and trend of high-capacitance multi-layer ceramic capacitor in Korea", Journal of the Korean Ceramic Society, vol 46, no. 2, pp. 161-169, 2009.

[2] Hyuk Sun, Zhe-Jun Jin, Myoung-Gyun Kim, Chan-Seo Park, and Tae-Yeoul Yun, "Equivalent-circuit modeling for multilayer capacitors based on coupled transmission-line theory", IEEE Trans. Comp., Packag., Techonl., vol. 1, no. 5, pp. 731-741, May 2011.

[3] A. T. Murphy and F. J. Young, "High frequency performance of multilayer capacitors", IEEE Trans. Microw., Theory Tech., vol. 43, no. 9, pp. 2007-2015, Sep. 1995.

[4] Johnson, Howard W., and Martin Graham. High-speed signal propagation: advanced black magic. Prentice Hall Professional, pp. 55-79, 2003.

[5] Grover, Frederick W. Inductance calculations: working formulas and tables. Courier Dover Publications, pp. 246-266, 2004.

[6] Plonsey, Robert, and Robert E. Collin. Principles and applications of electromagnetic fields. New York: McGraw-Hill, pp. 160-162, 1961.

[7] Paul, Clayton R. Analysis of multiconductor transmission lines. John Wiley &Sons, pp. 282-304, 2008.

★★★